# Measuring Hydrogen Pressure over a Palladium Bed

**Joseph Mastrandrea**
Webster Thomas High School
LLE Advisor: Walter Shmayda

**Abstract:**

       An experimental setup that utilized a Pd bed connected to a heater and a cryocooler, which operates according to the Stirling Cycle, was used to collect data on the formation of palladium hydride. Palladium is a member of a group of metals which have been found to absorb the different isotopes of hydrogen to form metal hydrides. Due to this, palladium is of interest on account of its ability to collect and store large volumes of hydrogen, deuterium, and tritium. Measuring the change in hydrogen pressure above the palladium at equilibrium at a fixed temperature provides the amount of hydrogen absorbed into the palladium. Pressure data was recorded for H/Pd ratios between 0.0 and 0.8 and temperatures between -40 C and 200 C. This extends the prior minimum temperature of study from 20 C to -40 C and expands the upper bound of the H/Pd ratio studied from 0.6 to 0.8. The absorption data indicates that palladium is an effective absorber of hydrogen at lower temperatures and can deliver hydrogen over a broad temperature range.

## Section 1: Introduction

The ability to form a hydride is a unique characteristic of palladium metal which makes it valuable in hydrogen collection processes. The focus of this particular experiment was on the formation of palladium hydride (PdH) at low temperatures. The study and understanding of the behavior of PdH at low temperatures is of importance at LLE because of its mission to study inertial confinement fusion reactions. The fuel delivery method employed during typical campaigns involves filling a cryogenic target, approximately one millimeter in diameter, with a mixture of deuterium ($D_2$) and tritium ($T_2$) in order to provide the fuel density required to create fusion conditions. In order to do this, a stock of gaseous tritium and deuterium must be kept for target charging purposes. Currently, the targets are being filled by permeation of DT through the outer plastic shell of the target (fig. 1). As the gas permeates through the outer skin, the pressure of DT inside the plastic shell increases until it is equal to the pressure surrounding it, at which point the target is full.
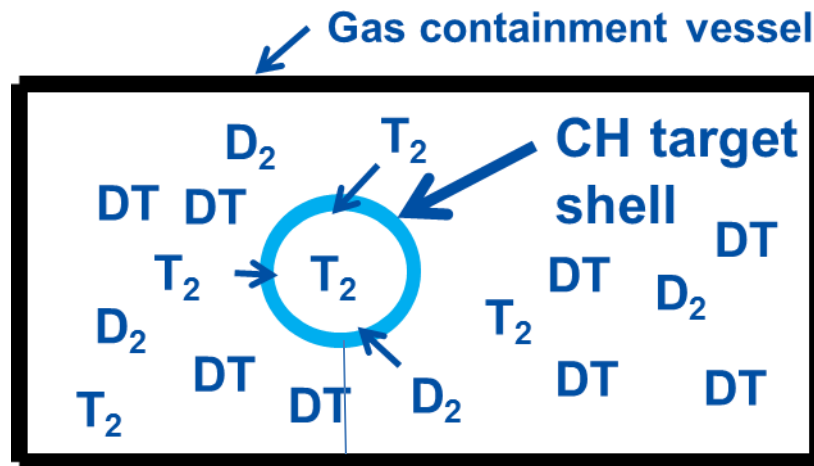


[Fig-1: Permeation filling process in which a target is filled with DT, $D_2$, and $T_2$ at high pressure]

Tritium is a radioactive gas, making it difficult to safely use in experiments and collect once released into the environment. Although this research was focused on the formation of palladium hydride, it can be extended to the hydrogen isotopes deuterium and tritium, forming palladium deuteride and palladium tritide, respectively. It is believed that heating palladium hydride to desorb the precise amount of gas required, and flowing the gas through a fill tube into

the plastic shell as shown in fig. 2, would be less damaging to the targets and simplify the method of target filling.
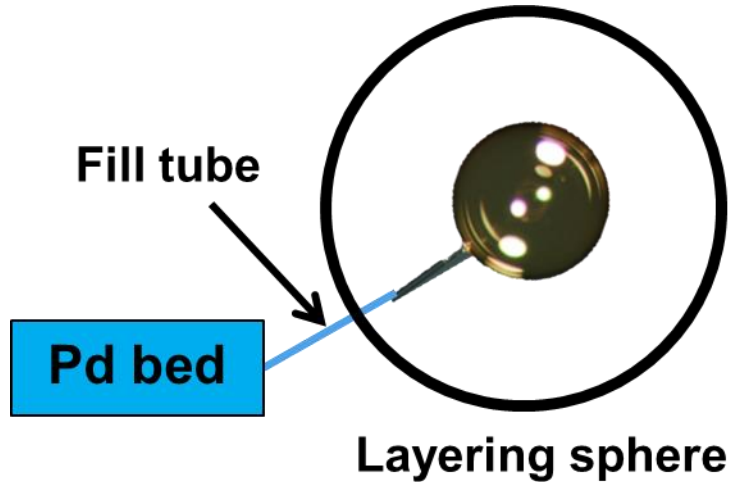


[Fig-2: Proposed less hazardous method of target filling using a palladium bed]

## Section 2: Theory and literature review

Palladium belongs to a unique group of metals which are capable of absorbing hydrogen into their lattice structure to form hydrides. This absorption process is complex and essentially occurs in three steps. This unique ability allows palladium to act as a hydrogen compressor, which means that palladium, at low temperatures, will absorb hydrogen resulting in a low vapor pressure above the metal. Then, upon heating, the vapor pressure of the hydrogen increases as it is desorbed from the palladium bed.

(2.1) Palladium hydride formation:

The hydrogen pressure over the palladium is plotted in fig. 3(a) against the ratio of hydrogen to palladium in the palladium bed at a number of temperatures. As hydrogen is introduced into the palladium bed at a given temperature, the vapor pressure above the palladium increases to form the Alpha ($\alpha$) region of the curve. Throughout this region, hydrogen atoms are dissolving into the palladium by fitting into the interstitial spaces within the hydrogen lattice in increasing quantities as the H/Pd ratio increases, as shown in the left part of fig. 3(b). At the end of the Alpha region, energetic favorability shifts from spontaneous absorption of hydrogen atoms into the lattice structure, to reactions with the palladium to form palladium hydride. This continues throughout the two-phase region ($\alpha$ & $\beta$), so called because there is both bonded and

3

dissolved hydrogen. As the hydrogen atoms introduced in each successive loading react to form palladium hydride and the H/Pd ratio increases, the reaction approaches the end of the two-phase region. At the end of the two-phase region, all of the palladium has been reacted to form palladium hydride, meaning that any further hydrogen introduced into the palladium bed is forced into solution within the newly formed palladium hydride lattice. This phenomenon continues throughout the Beta ($\beta$) region until all of the spaces within the palladium hydride lattice are full and no additional hydrogen can be absorbed. With increasing temperature, the length of the two-phase region of the isotherm decreases until $T_c$ is reached after which point there is no extended two-phase region. This is due to the fact that the formation of PdH is an exothermic process and is slowed as the temperature of the palladium is increased.

(a)



(b)

α Region          Two Phase          β Region
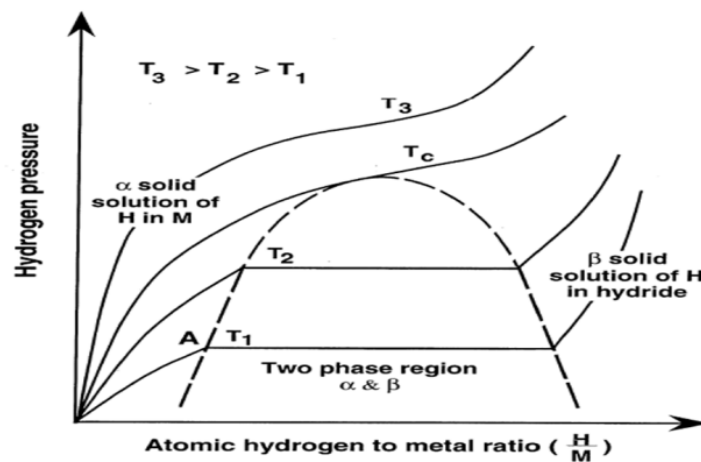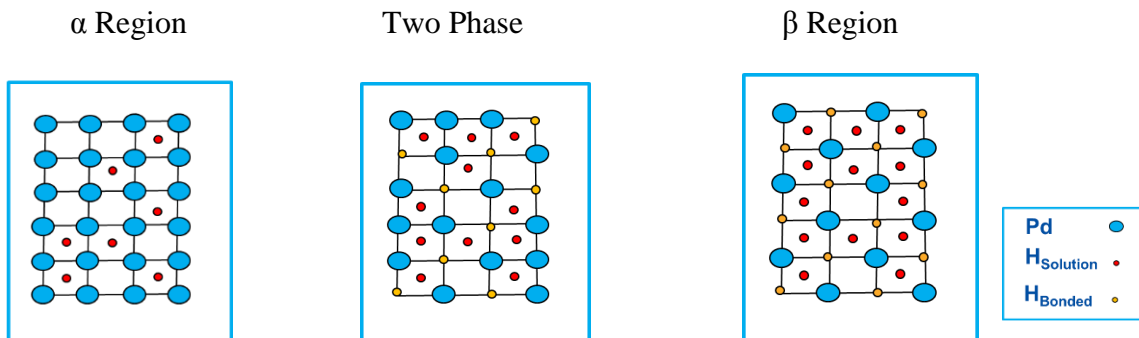


[Fig-3: (a) Phase diagram of PdH isotherms at increasing temperatures from $T_1$ to $T_3$. (b) Structure of PdH in each of the three phases]

4

(2.2) Prior published research:

Previous research has shown a trend toward increased hydrogen pressure above a palladium bed as temperature is increased. This phenomenon is illustrated in figure 4, which is Gillespie's [Ref. 2] plot of isotherms between 20 C and 298 C. From this plot, it can also be observed that the length of the two-phase region decreases with increasing temperature, as in fig. 3.
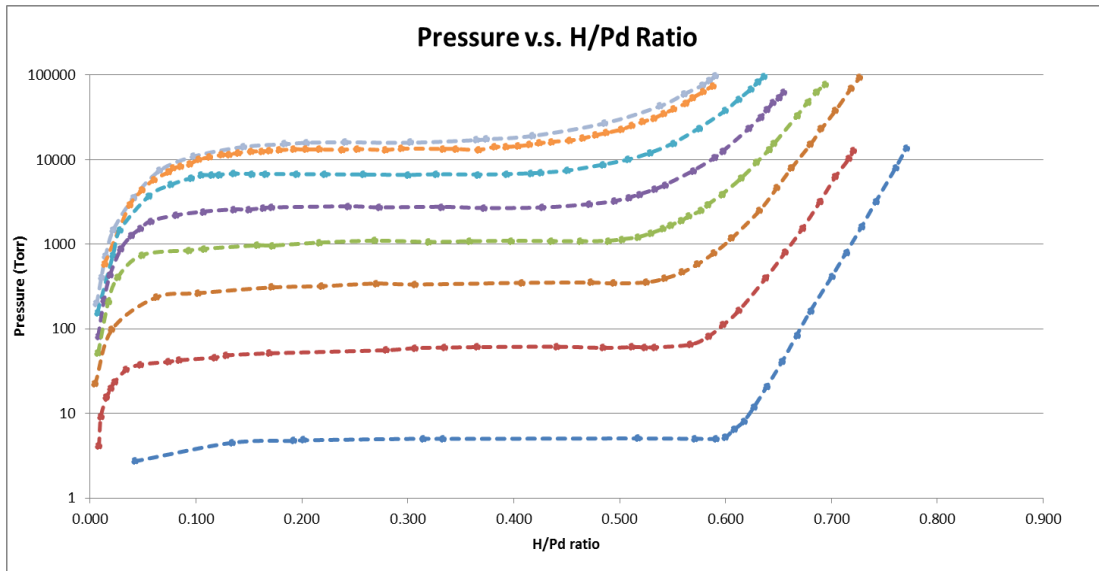


[Fig-4: Isotherms from Gillespie[2] for the pressure of hydrogen above a Pd Bed. Temperatures range from 20 C (bottom) to 298 C (top)]
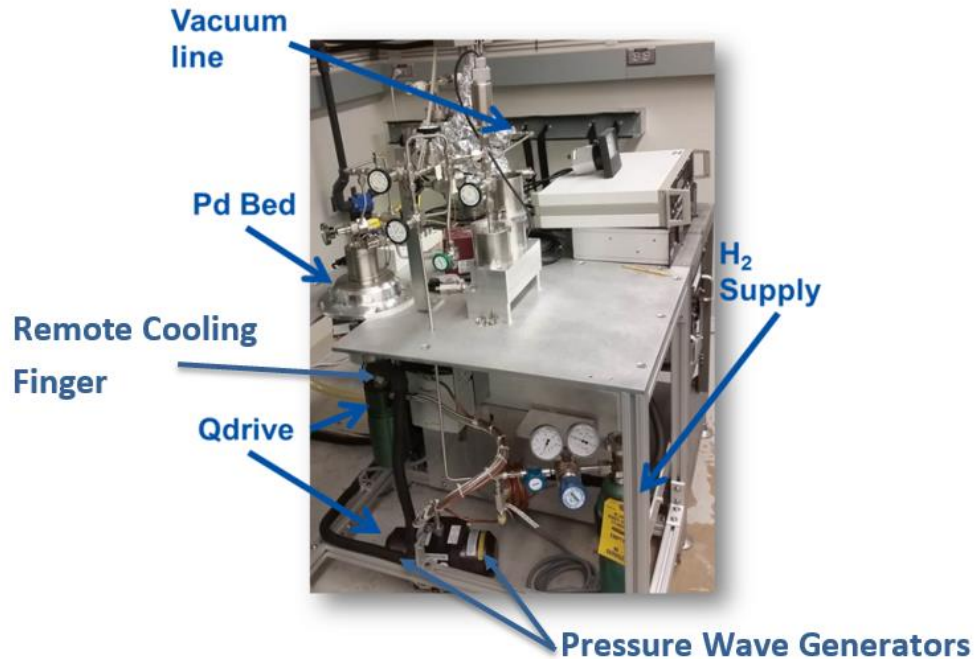
## Section 3: Experimental setup

The experiment was designed to study the formation of PdH at lower temperatures: 20 C and below. A vacuum system was constructed to introduce hydrogen in discrete steps into an evacuated bed containing palladium powder so that the mass of hydrogen delivered to the bed could be measured. Between 10 and 14 psia of hydrogen was flowed through evacuated tubing from the hydrogen supply to the Pd bed as shown in Fig. 5. Each charge of hydrogen was isolated between the valves $V_{Pd}$ and $V_1$ before the bed was opened, to ensure that the initial pressure could be precisely measured. The measurement was taken using an MKS capacitance manometer measuring in Torr.

The experimental setup of figure 5 was designed to introduce a precisely measured quantity of hydrogen gas into the palladium bed. The palladium bed was surrounded by an evacuated secondary containment maintained between $10^{-6}$ and $10^{-7}$ Torr by a turbomolecular drag pump (labeled VAC in fig. 5). Vacuum pressures were measured with an ion gauge while the pressure of the hydrogen used to charge the system was measured using the two pressure transducers. For each step of the loading, hydrogen was introduced through the hydrogen supply line into the space between $V_{iso}$, $V_{Pd}$ and $V_{Hydrogen}$, where the pressure was measured prior to the Pd bed being opened. This cycle was repeated multiple times for each complete loading of the Pd bed.
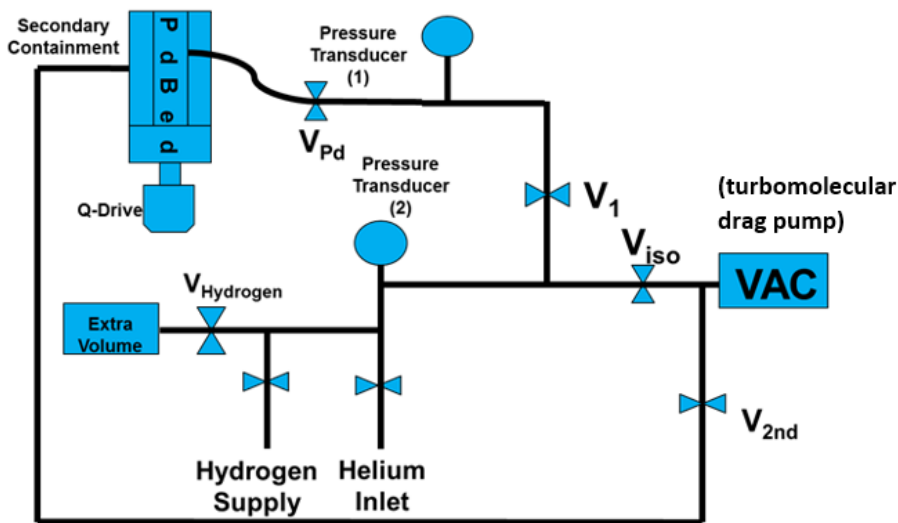


[Fig-5: Schematic of the experimental setup for introducing precisely measured quantities of hydrogen gas into a Pd bed]

In order to maintain isothermal conditions in the palladium bed, a Qdrive cryocooler was attached to the bottom of the Pd bed and all lines were evacuated with a turbomolecular vacuum pump to prevent air or water contamination from the surroundings. The hydrogen pressure measurements were taken using capacitance manometers (represented by pressure transducers 1 and 2 in fig. 5) and the vacuum pressure measurements were made using an ion gauge (near the intake of the vacuum pump at VAC in fig. 5) ensuring the highest level of precision. Figure 6 is an image of the experimental setup that is characterized by the above schematic.

[Fig-6: The experimental setup including vacuum system and electronics]

(3.1)  Palladium bed:

Inside the palladium bed (fig. 7) is 2.5 grams (.0235 mol) of palladium sponge, which is contained within a stainless steel vessel with a free volume of 5.38 cc. The bed is contained in a large stainless steel cylinder connected to the turbomolecular vacuum pump that maintains a vacuum between $10^{-6}$ and $10^{-7}$ Torr. The vacuum is necessary to prevent ambient heat from entering and affecting the temperature inside the bed. Having highly resistive insulation is especially important as the focus of the experiment was on hydride formation at temperatures below 20 C. Additionally, at temperatures as low as -100 C, the rate of absorption of ambient heat is greater due to a greater temperature gradient between the Pd bed and the surrounding air, so thorough insulation is of great importance for good temperature control.
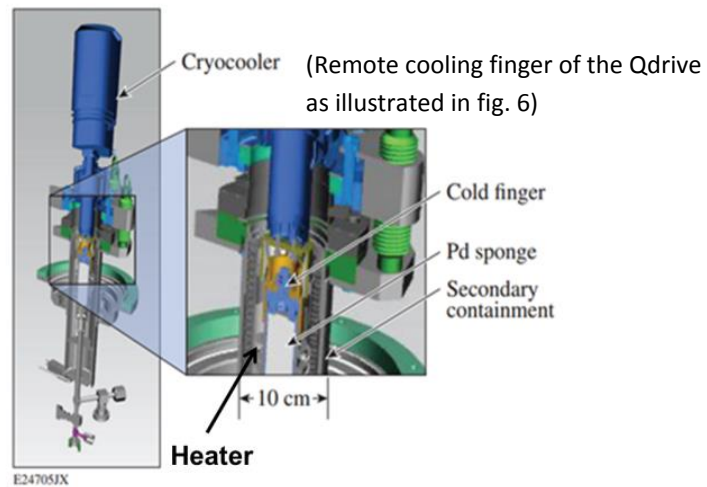
[Fig-7: Pd bed, thermally isolated by an evacuated secondary containment. The temperature is controlled with a Qdrive cryocooler and a trim heater]

(3.2) Qdrive and Stirling cycle:

The Qdrive is a cryocooler which has a remote cooling finger attached to the bottom of the palladium bed, as shown in fig. 5, maintaining thermostatic conditions within the bed. As shown in fig. 8, the Qdrive uses a closed system of compressed helium (25 bar) which is passed through a series of heat exchangers in the cold head. The helium is forced through the heat exchangers and regenerator, labeled warm HX, cold HX, and regenerator in figure 8, under pressure generated by the pressure wave generators (PWG). These heat exchangers are all located in the cold head of the Qdrive, which is filled with the pressurized helium. The regenerator allows for the heat to be drawn from the helium to the cooling water with each cycle of the PWGs as it pumps the heat out of the helium into the cooling water. Each PWG is a linear motor connected to a piston, and as the piston is driven into the space containing the helium, the volume decreases, therefore increasing the pressure. In the Qdrive, the pressure wave generators are designed to oppose each other so that greater helium pressure can be achieved and vibration limited as each movement of a piston is opposed by that of the other piston to avoid colliding with each other.
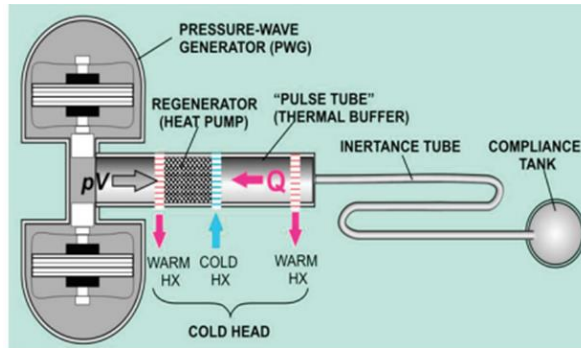
[Fig-8: Cross section of a Qdrive, which is a compressed helium, Stirling cycle, cryocooler. Image from www. Chartindustries.com]

The Qdrive operates according to the principle of the Stirling Cycle which has four main thermodynamic steps beginning with an isothermal compression of the gas (from a to b in fig. 9) followed by an isochoric cooling of the gas (from b to c in fig. 9). Next is an isothermal expansion of the gas (from c to d in fig. 9). The final step is an isochoric heating of the gas (from d to a in fig. 9) after which the cycle repeats.
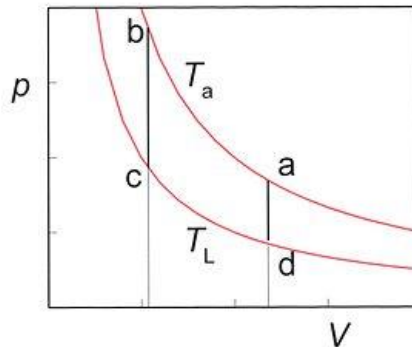


[Fig-9: Paths in the (P,V) plane taken by the He gas in a Qdrive cryocooler. The curved paths are isotherms. Image source: google images]

Inside the Qdrive, the cycle begins in stage 1 with the compression of the helium gas through the cold heat exchanger and into the pulse tube as the PWGs move towards each other. The helium is then forced into the inertance tube (see Fig. 8), where its velocity increases due to the smaller diameter of the opening to the tube relative to the diameter of the pulse tube. Due to the inertia of the helium and its momentum out the inertance tube, as well as its higher velocity towards the compliance tank, the helium undergoes the expansion step of the Stirling Cycle. As the helium expands, it absorbs the heat from the cold head which is attached to the palladium

9

bed. When the PWG's reverse directions, the helium is drawn back to the pulse tube through the hot heat exchanger, dissipating the heat from the helium before the cycle repeats.

(3.3) Ion gauge:

The quality of the vacuum was measured using an ion gauge (fig. 10) driven by a Granville-Phillips 307 Vacuum Gauge Controller to obtain readings in the high vacuum region. The ion gauge uses a filament which, upon heating, thermionically emits electrons into an electric field, accelerating them, and providing them with the energy required to ionize any gas molecule within the cylindrical space defined by the grid. A wire called the collector runs down the middle of the grid and carries the current generated by the positively charged gas ions inside the grid volume. That current is directly proportional to the pressure of the gas inside. The ion gauge was used to measure the vacuum when gas pressures were below $10^{-3}$ Torr.
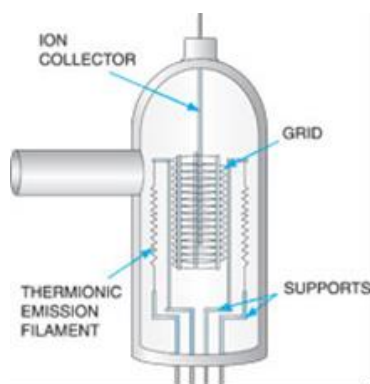


[Fig-10: Ion gauge used to measure pressures in the high vacuum range]

(3.4) Capacitance manometer:

Initial and final hydrogen pressures were measured with an MKS Baratron pressure transducer, which utilizes a capacitance manometer (fig. 11), in the pressure range 0.01 to 800 Torr. This particular manometer is rated to measure over a pressure range of 0 to 1,000 Torr. The pressure measurements taken in these experiments were, therefore, well within the acceptable operating range of the device.
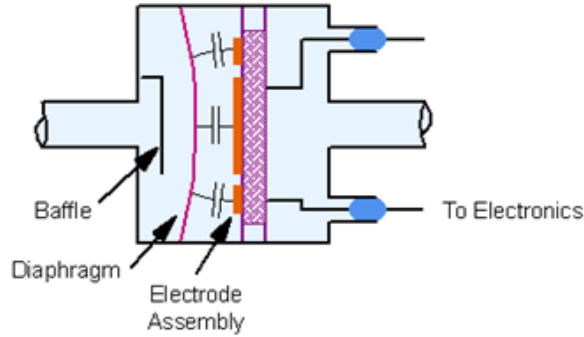
[Fig-11: Capacitance manometer used to measure accurately across multiple decades of pressure]

A capacitance manometer contains an air-gap capacitor that has one electrode attached to the stainless outer case and another attached to an interior diaphragm. Under increasing pressure from the input piping to the gas source being measured, the diaphragm deforms inward and the air gap between the two electrodes of the capacitor decreases, thereby decreasing the capacitance. Contained within the same circuit as the diaphragm are an oscillator and a demodulator, which measure the capacitance while the MKS Type 670 Signal Conditioner records the readings. The capacitance manometer is efficient at recording hydrogen gas pressure because the design is insensitive to gas species and can be configured to be linear over a broad pressure range.

(3.5) Turbomolecular drag pump:

A turbomolecular drag pump (fig. 12) was used to evacuate all of the 1/4" dia. stainless steel piping within the system to pressures between $10^{-6}$ and $10^{-7}$ Torr to remove any impurities that may have entered from the surroundings. The turbomolecular drag pump uses between 10 and 40 different stages of blades to compress the input gas and remove it from the vacuum system. Each stage consists of a rotor and a stator pair, with the rotor spinning between 9000 and 90,000 rpm. The stator deflects the molecules propelled by the rotor into the next stage to compress the volume of air towards the exhaust. This pattern repeats as the gas travels through the pump until it is expelled from the exhaust. Turbomolecular pumps are capable of pumping between 100 and 800 liters per second. This pump was run continuously to ensure that the secondary containment of the Pd bed and all of the piping were evacuated and the system was rid of any leftover hydrogen gas from prior loadings.
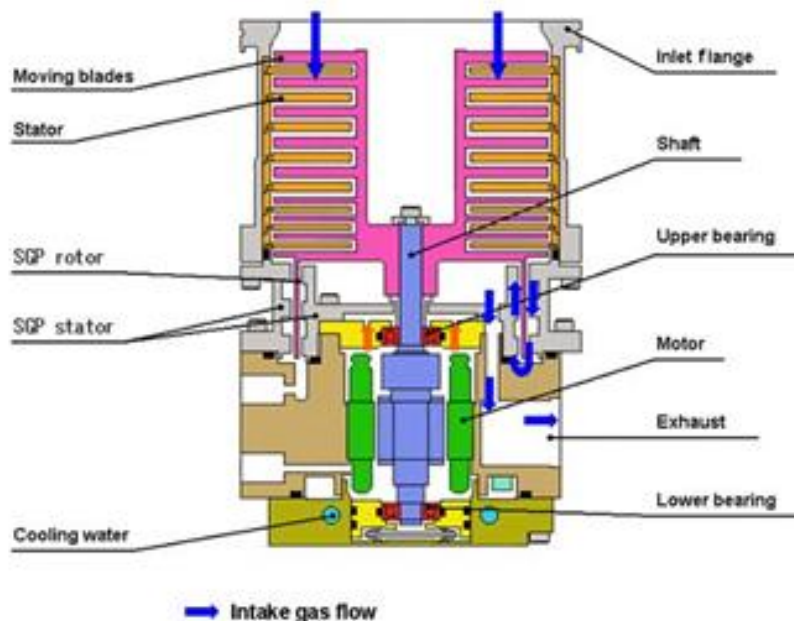
[Fig-12: Turbomolecular drag pump used to evacuate the system to between $10^{-6}$ and $10^{-7}$ Torr]

## Section 4: Procedure

(4.1) Loading the palladium bed:

The palladium bed (fig. 5) was loaded in a stepwise fashion, allowing each known mass of hydrogen released into the bed to reach equilibrium. To measure the mass of hydrogen introduced into the bed, 18.2 cc of piping was loaded with hydrogen at 297 K and the pressure recorded. The pressure was adjusted to control the amount of gas desired for each loading but ranged from 3.8 to 13.8 psi (200 to 713 Torr). When the valve to the palladium bed was opened, the gas flowed into the bed and was absorbed into the palladium sponge until equilibrium was established, at which point the palladium bed was isolated and the pressure in the hydrogen line was recorded again. This process was repeated for each loading. Initial and final pressure measurements provided the equilibrium vapor pressure and allowed the mass of hydrogen introduced and the hydrogen to palladium ratio to be calculated for each loading.

12

(4.2) Unloading in steps:

In order to unload the bed in steps, all lines connected to the palladium bed were evacuated to $10^{-6}$ Torr. The expansion volume was then isolated from the vacuum pump. Connected to the Pd bed, the expansion volume is composed of the piping from the bed to the tank labeled extra volume (see Fig-5), yielding a total volume of 544.8 cc when $V_{iso}$ is closed. A larger volume was necessary to remove any additional gas during each step in order to expedite the unloading. Secondary containment of the palladium bed was open to the vacuum pump at all times except when the hydrogen was being pumped out of the expansion volume. The reason for this was to prevent hydrogen entering the secondary containment volume and creating a thermal short. Once the pressure inside the expansion volume stabilized and the palladium bed reached equilibrium, the bed was isolated and the pressure in the expansion volume was measured. Doing so provided data on the mass of gas removed from the bed and on the change in the hydrogen/palladium ratio. Following this, the secondary containment was isolated from the vacuum pump and the expansion volume was evacuated to $10^{-6}$ Torr. This process was repeated for each step of the unloading to collect the data for each isotherm.


(4.3) Unloading by heating:

To clear the bed of all hydrogen prior to each run, the palladium bed and all of the hydrogen lines were evacuated. To enable this, the ion gauge was powered down to avoid burning out the filament from exposure to the high gas pressures (above $10^{-3}$ Torr) released from the hydrogen supply lines. Next, the palladium bed and secondary containment vessel were isolated by closing $V_{Pd}$ and $V_{2nd}$. Lastly, the valve to the vacuum pump was opened allowing the turbomolecular vacuum pump to remove the gas and evacuate those lines to below 1 Torr. Following this, $V_{Pd}$ was opened and the hydrogen began to desorb from the palladium sponge. Once the pressure reading from the bed dropped below 0.3 Torr, the Qdrive was turned off and the temperature of the bed was raised in 10 to 20 degree increments to 200 C. The temperature of the bed was left at 200 C overnight to ensure desorption of all hydrogen from the palladium and to establish a hard vacuum ($10^{-6}$ Torr) in all of the lines and the palladium bed. Once this was achieved, the temperature was decreased towards the desired temperature for the next loading by reducing the heat source. When the temperature dropped below 120 C, the Qdrive was re-

enabled, allowing the bed to be cooled to the new starting temperature. Once the temperature of the bed stabilized at the desired value, the palladium bed was isolated by closing $V_{Pd}$ and opening $V_{2nd}$ to evacuate the secondary containment vessel and insulate the bed from the environment. At this point, the system was ready for the palladium bed loading procedure to begin again.

## Section 5: Data

(5.1)  Experimental results:

For each loading of the palladium bed, pressure, bed temperature and H/Pd data were recorded.  Isotherms were plotted on a hydrogen pressure versus hydrogen to metal ratio graph (fig. 13) to study the vapor pressure of hydrogen above the palladium sponge throughout the hydride formation process. Loadings were made from -40 C to 200 C. The data shown in Fig 13 reveal that the hydrogen vapor pressure increases as the palladium temperature is increased. From this observation, it was concluded that palladium will compress hydrogen well below 423 K (150 C) and throughout the two-phase region which extends from H/Pd ratio of 0.1 to 0.6. The length of the two phase region of each isotherm varies with temperature, providing an experimental illustration of the behavior shown in figure 3.
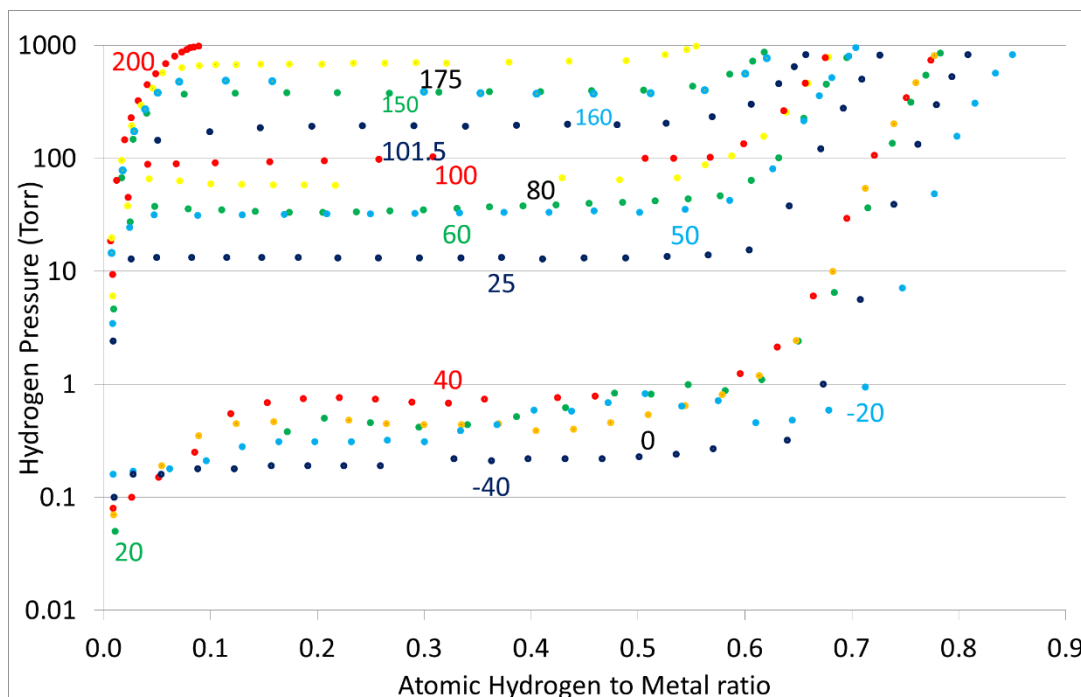
[Fig-13: Isotherms returned by this study with temperatures ranging from -40 C to 200 C]

The 25 C isotherm has a two-phase region of higher equilibrium pressure than the 40 C isotherm, which should not be the case. The probable cause of this could be premature pressure measurements made before the reaction reached equilibrium during the 25 C loading. Additionally, the low pressure of the two-phase region of the 40 C isotherm could be due to temperature fluctuations during the loading that may have caused the vapor pressure of the hydrogen over the palladium bed to decrease beyond expected the equilibrium for that temperature.

As the temperature of the isotherm increased, a decrease in the length of the two-phase region was observed. The theoretical limit to form palladium-hydride in the palladium hydrogen system occurs at PdH, that is to say one hydrogen for every palladium atom. At higher temperatures, it is energetically more favorable to dissolve hydrogen in palladium hydride when the H/Pd ratio is between 0.5 and 0.6. However, the data shows that as the temperature of the metal decreases below 20 C, the tendency to form palladium hydride beyond H/Pd ~ 0.6 is favored relative to dissolving hydrogen in the hydride because the H/Pd ratio at which the plot curves up after the two-phase region increases with decreasing temperature. The lower isotherms

15

shown in Fig. 13 indicate that the quantity of hydrogen that palladium is capable of capturing and storing increases as the temperature of the palladium decreases due to the longer two-phase region of the plot.

Each of the loadings was repeated to demonstrate the consistency with which the isotherms could be reproduced. Figure 14 provides examples of three sets of data taken at -20 C. Each data set indicates that the two-phase region spans a H/Pd range from 0.1 to 0.65, and an equilibrium pressure of approximately 0.2 to 0.5 Torr over that range.
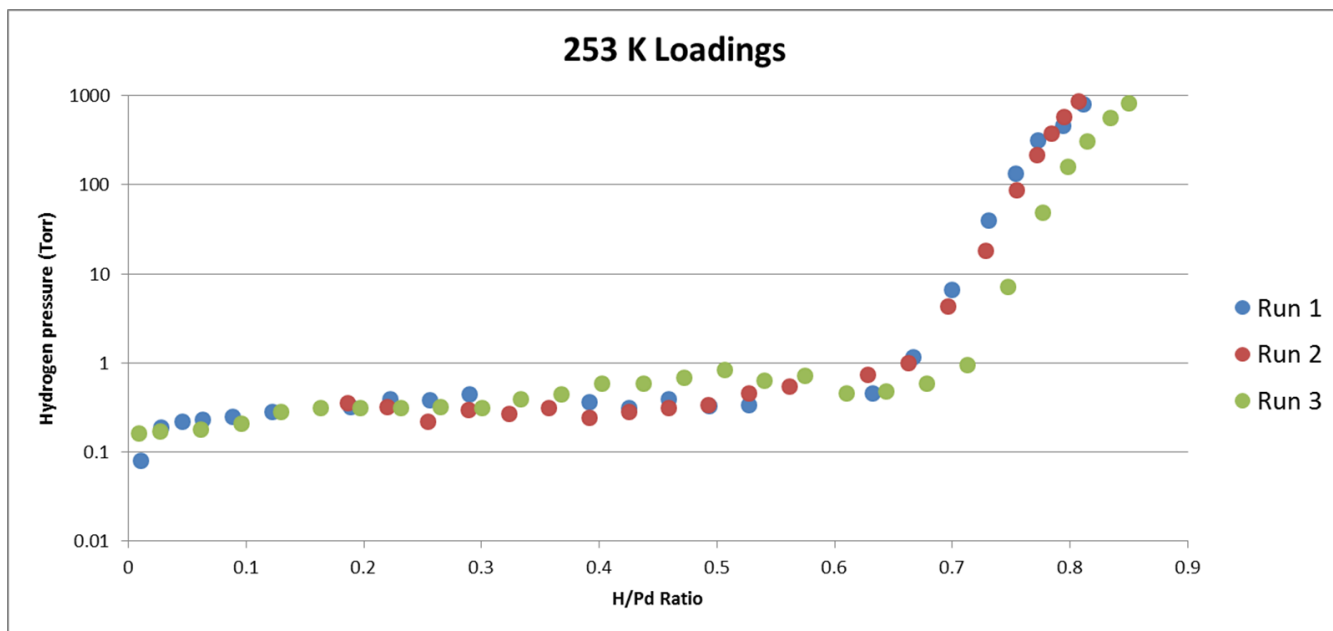


[ Fig-14: Three isotherms at -20 C, confirming reproducibility]

(5.2) Van't Hoff curves:

To describe the vapor pressure dependence in the two-phase region, a mathematical relationship was needed to relate the temperature of the palladium bed to the vapor pressure of hydrogen above it. The Van't Hoff equation shown below (equation 1) was used.

The Van't Hoff equation relates the natural log of pressure, ln(P), to the enthalpy of formation of palladium hydride, $\triangle$Hf, and the entropy of formation, $\triangle$Sf, of palladium hydride for any given isotherm at temperature T. R is the ideal gas constant. The Van't Hoff equation was simplified by substituting constants A & B as shown in equation 2. The constant A represents the enthalpy of formation of palladium hydride divided by the ideal gas constant. The constant B represents the entropy of formation of palladium hydride divided by the ideal gas constant.

$$\ln(P) = \frac{-\boldsymbol{\Delta Hf}}{RT} + \frac{\boldsymbol{\Delta Sf}}{R} \qquad (1)$$

$$\ln(P) = \frac{-A}{T} + B \qquad (2)$$

To determine the constants A and B, plots were constructed of pressure dependence against inverse temperature using data from the two-phase region across each of the distinct isotherms at several fixed H/Pd ratios. As shown in Fig. 15, for two mole ratios 0.21 and 0.50, the data for each temperature were compiled on a plot of ln(P) versus 1/T. A best-fit line was then regressed returning the best-fit A and B coefficients.
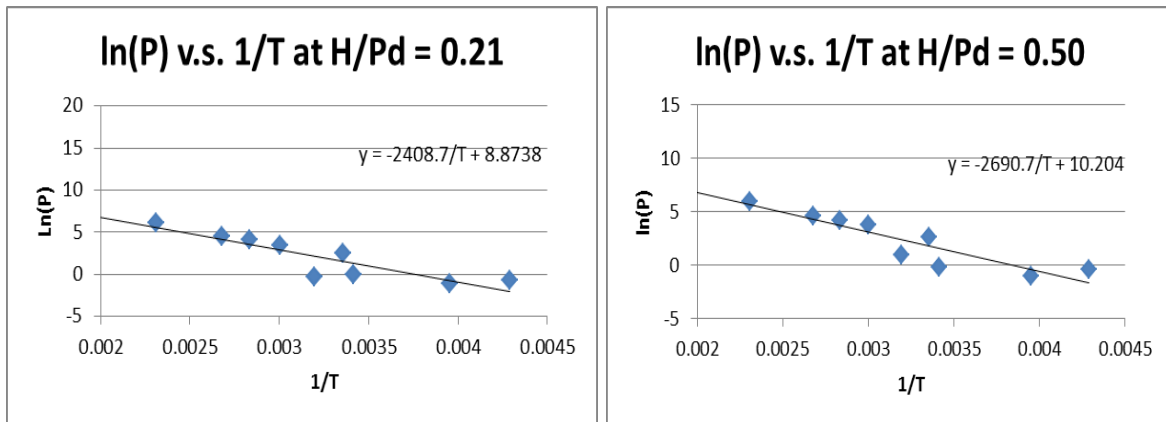


[Fig-15: Van't Hoff curves for H/Pd ratios of 0.21 (left) and 0.50 (right), showing a linear relationship across the length of the two-phase region]

Pressure measurements at H/Pd = 0.21 were chosen because that ratio was common for the majority of the isotherms due to the quantity of gas added during each step of each loading.

The two sets of coefficients returned by these plots reveal the degree of correlation for the exponential fit for the two-phase region of the plot at the two extremes of the H/Pd ratios studied. It is noteworthy that the constants for the two cases are similar.  The slight increase in the two constants for the higher H/Pd value is consistent with the observation that the slope of the plateau region between 0.2 and 0.5 is not zero but increases slightly as the H/Pd ratio increases.

(5.3) Comparison with prior research:

Table 1 is a compilation of the data collected by previous researchers. This table includes the A and B constants as well as the temperature range over which isotherms were obtained. The constants returned by this study are close to those of previous experiments, although some variation is evident. This variation could have been the result of the significantly wider temperature range undertaken by this experiment. Alternately there may have been outliers on certain isotherms at the H/Pd ratios sampled to construct the Van't Hoff plots. Such values could have resulted from pressure measurements taken prior to equilibrium, or an environmental factor causing unstable temperatures, especially at the extreme ends of the temperature range.

| Author | A (K) | B | Temp. Range (K) |
|---|---|---|---|
| Wicke and Nernst[4] | 2039 | 7.65 | 195 to 323 |
| Gillespie and Hall[6] | 1878 | 7.48 | 273 to 453 |
| Ratchford and Castellan[5] | 2028 | 7.98 | |
| This study | 2409 | 8.87 | 233 to 473 |

Table 1: Comparison of constants derived from this study against values published in the literature

Figure 16 plots the pressure-temperature relationship given by Eq. 2 using the Van't Hoff constants from this study and those of the other researchers. The present curve is consistent with the findings of the prior research, although characterized by a slightly steeper slope. Overall, the variability observed between the Van't Hoff constants of this study and those of prior research was not found to be statistically significant.
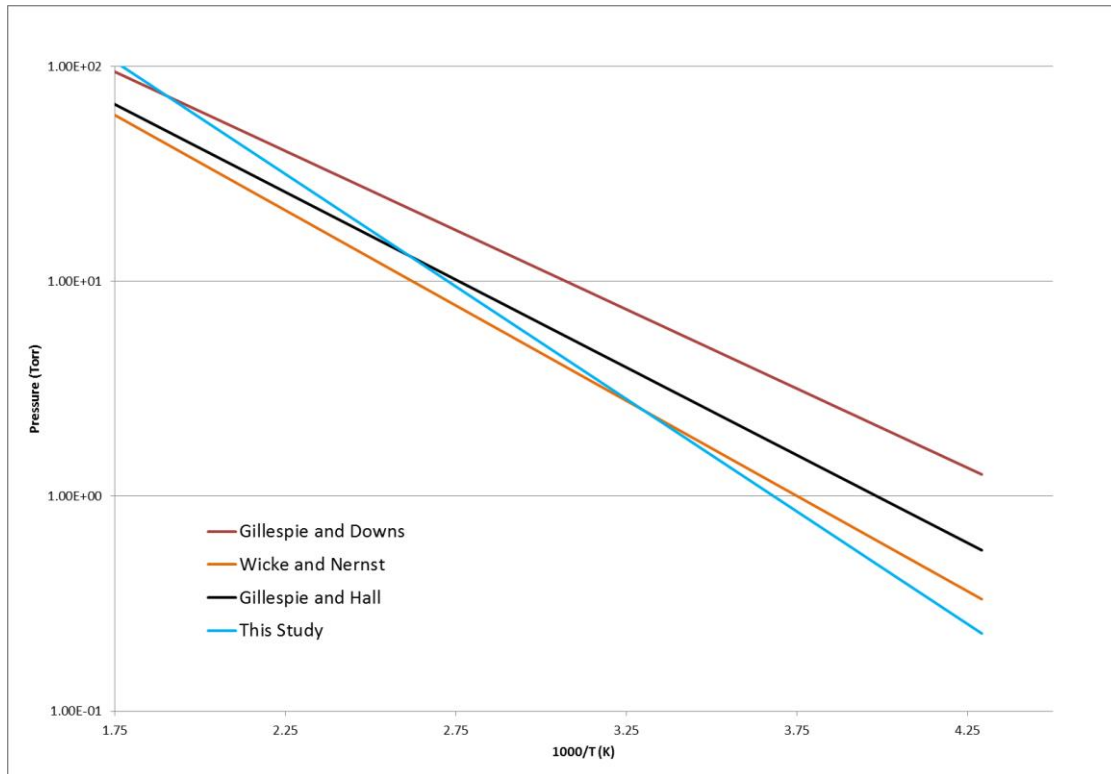
[Fig-16: Dependence of pressure on temperature based on the Van't Hoff constants obtained from previous studies and this study]

The Van't Hoff curve also allows for a comparison between palladium and other hydrogen-compressing metals. In Fig. 17, the Van't Hoff curve for uranium is plotted along with the curves for palladium to illustrate that uranium must be heated to significantly higher temperatures to achieve comparable hydrogen vapor pressures with palladium. The fact that uranium provides lower vapor pressures at low temperatures indicates that uranium is better suited for longer-term hydrogen storage than palladium.  However, palladium is better suited as a hydrogen compressor because higher pressures can be attained at lower temperatures compared to uranium. Compressing tritium at lower temperatures means that less tritium will permeate through the containing vessels. Additionally, palladium is better suited to deliver tritium to targets because it desorbs the hydrogen at lower temperatures, allowing less stress on the cryogenic cooling equipment and easier maintenance of the temperature of the target.
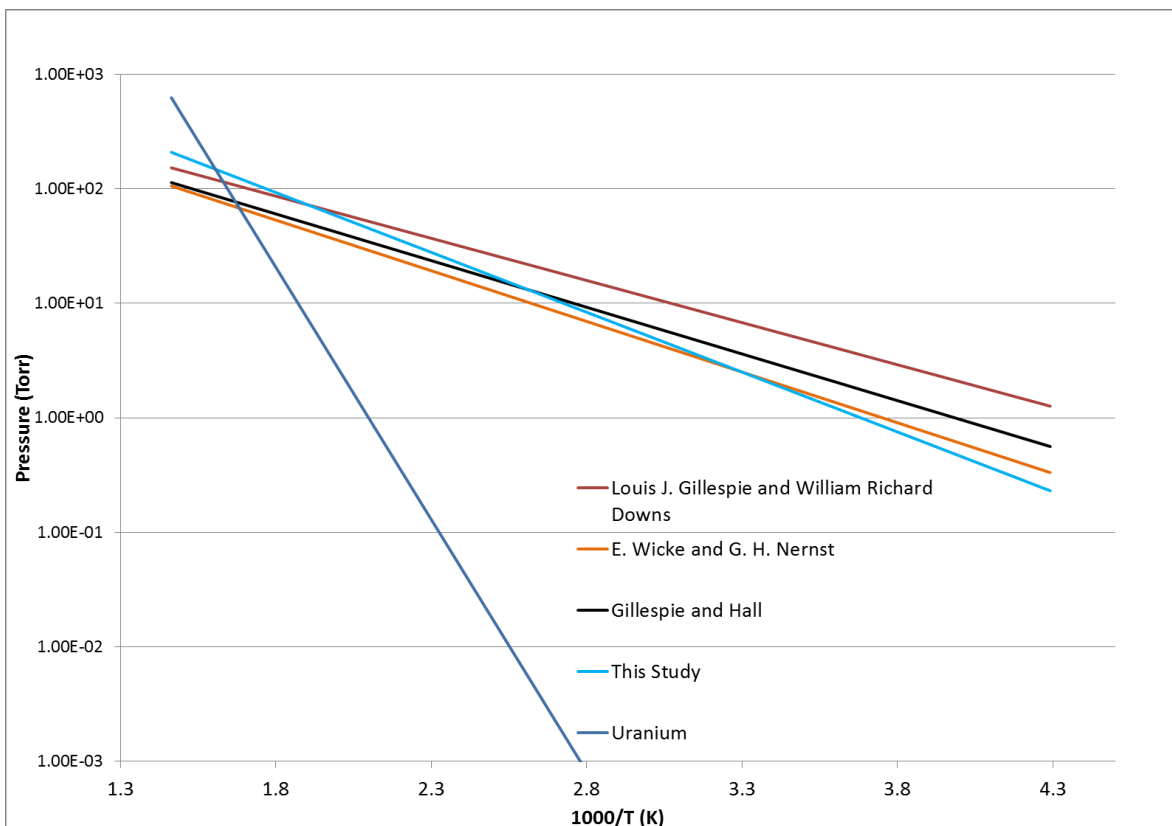
[Fig-17: As figure 16 except that data for uranium has been added. Gas is desorbed from palladium at lower temperatures than for uranium]

## Section 6: Discussion and Conclusions

Though the data correlated well with the results of prior experiments, there were slight differences between the Van't Hoff constants returned by this study and those of prior research. One of the potential causes for this variation in the results could have been temperature non-uniformity throughout the palladium bed.
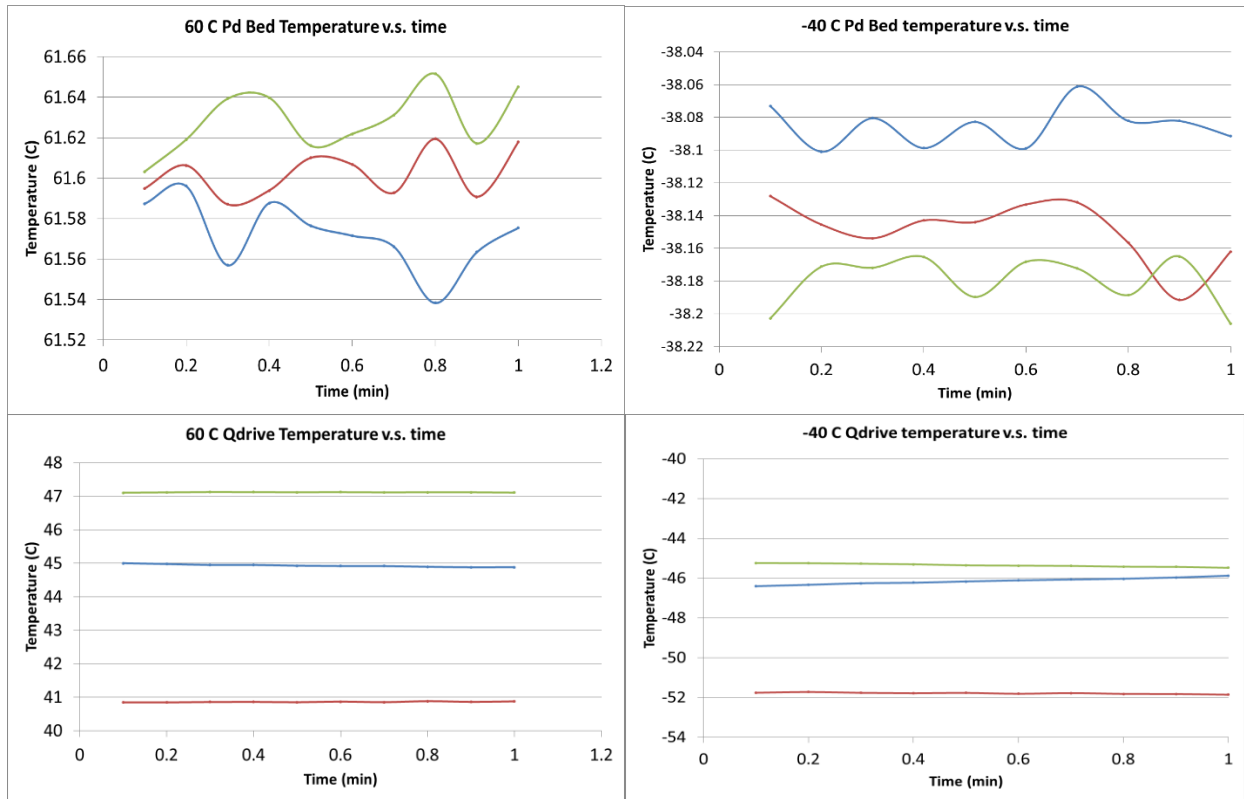
[Fig-18: Temperature of the Pd bed (top) and Qdrive (bottom). Temperature measurements from the Pd bed versus time for 3 loadings at 60 C (left) and -40 C (right), demonstrate temperature variability of the Pd bed. There was difficulty maintaining completely thermostatic conditions in the Pd bed with the Qdrive and the trim heater opposing each other]

The plots in Fig. 18 indicate the temperature flucuations that were present in the palladium during a given step of a loading with each line representing the rate of change of the palladium bed during that particular step. Each color line is plotted with the temperature readings from the thermocouples at the Qdrive and Pd bed at 60 and -40 C, respectively. Each line shows a varying slope which indicates that throughout each step, the temperature changed but at a different rate from step to step. Such fluctuations in the temperature of the palladium bed are likely the result of the Qdrive opposing the trim heater. This effect became more apparent at the outer bounds of the temperature range studied. Figure 18 shows an approximately 7 degree spread in the Qdrive temperatures for the three loadings performed at -40 C. Based on the plots in Fig. 18, the variation in equilibrium pressures in the two-phase region between multiple loadings at a particular temperature is most likely due to the fact that the Qdrive temperature varied between, as well as during, each loading. This effect may also have contributed to the

length of time required for the reaction to equilibrate in the two-phase region, resulting in pressure readings being taken too early.

Overall, based on the data returned by this study, it can be concluded with a high degree of confidence that palladium is a good compressor of hydrogen at lower temperatures. In addition, the fill-tube method for charging targets by desorbing hydrogen from a palladium bed would be a safe and viable alternative to the current method of permeation filling with a gaseous mixture.

## Section 7: Acknowledgements

## References:

1: D. H. W. Carstens and W. R. David. Equilibrium Pressure Measurements in the Beta region of Palladium Protide and Palladium Deuteride. National technical Information Service. March 1989

2: L. J. Gillespie and W. R. Downs. The Palladium-Deuterium Equilibrium. Research Laboratory of Physical Chemistry, Massachusetts Institute of Technology. Jul 10, 1939

3: F. D. Manchester, A. San-Martin, and J. M. Pitre. The H-Pd (Hydrogen palladium) System. Journal of Phase Equilibria. (15, 1) 1994

4: E. Wicke and G. H. Nernst. Zustandsdiagramm und thermodynamisches Verhalten der Systeme Pd/H2 und Pd/D2 bei normalen Temperaturen; H/D-Trenneffekte. Institut fur Physikalische Chemic der Universitat Munster. Nov 26, 1963

5: Mueller, Blackledge, and Libowitz. Metal Hydrides. Academic Press. Pg 641-3. 1968

6: L. J. Gillespie and F.P. Hall, The Palladium-Hydrogen Equilibrium and Palladium Hydride, American Chemical Society (1964)